PHYSICAL REVIEW B **81**, 041312(R) (2010)

Semiconductor-homojunction induction in single-crystal GaN nanostructures under a transverse electric field: *Ab initio* calculations

Hulusi Yilmaz,[1,2] Brad R. Weiner,[1,3] and Gerardo Morell[1,2]
[1]*Institute for Functional Nanomaterials, University of Puerto Rico, San Juan, Puerto Rico*
[2]*Department of Physics, University of Puerto Rico, San Juan, Puerto Rico*
[3]*Department of Chemistry, University of Puerto Rico, San Juan, Puerto Rico*
(Received 28 October 2009; published 29 January 2010)

Ab initio calculations show that a transverse electric field induces a homojunction across the diameter of initially semiconducting GaN single-crystal nanotubes (SCNTs) and nanowires (NWs). The homojunction arises due to the decreased energy of the electronic states in the higher potential region with respect to the energy of those states in the lower potential region under the transverse electric field. Calculations on SCNTs and NWs of different diameters and wall thicknesses show that the threshold electric field required for the semiconductor-homojunction induction increases with increasing wall thickness and decreases significantly with increasing diameter.

DOI: 10.1103/PhysRevB.81.041312 PACS number(s): 73.63.−b, 73.61.Ey

GaN is an important material for the applications in high-power/high-temperature electronics and potential blue-uv light emitting devices.[1,2] A distinct aspect of GaN is that, apart from its low-dimensional structures—such as nanowires (NWs),[3–6] nanodots,[7] and thin films[8]—it can also be synthesized in single-crystal nanotube[9–11] (SCNT) form. These SCNTs are similar to the NWs grown in the [0001] direction with a hexagonal cross section and [10−10] facets, but they have an axial hexagonal hollow region. The inner diameter of these SCNTs, synthesized in the "epitaxial casting" approach,[9] ranges from 30 to 200 nm and their wall thickness varies from 5 to 50 nm.

In this Rapid Communication, we report the feasibility of switching the band gap of GaN SCNTs and NWs under a transverse electric field. In device physics, the transverse electric field resembles a gate voltage applied to a channel through an insulating substrate. This band-gap switching mechanism with the external electric fields may open new areas for these nanostructures in the applications involving electronic and optoelectronic devices. An example of such a device is a field effect transistor based on a single-crystal *n*-type GaN NW, fabricated by Huang *et al.*,[12] who showed that the device exhibits good switching behavior with the modulation of conductance by more than three orders of magnitude. There have been similar attempts,[13,14] within the same approach, to utilize single-wall carbon nanotubes (CNTs) as switching nanodevices. However, despite the recent progress,[15] the separation of the semiconducting CNTs from the simultaneously grown metallic ones is difficult. On the other hand, GaN SCNTs and NWs have the advantage of being synthesized purely in semiconducting phase.

Using theoretical methods, band-gap switching under the transverse electric fields has been predicted for semiconducting CNTs,[16–18] boron nitride nanotubes (BNNTs),[19,20] and zigzag graphene nanoribbons (ZGNRs).[21–24] However, these studies have reported a semiconductor-metal (half metal for ZGNR) transition. The results presented here for GaN nanostructures, on the other hand, show that the conductivity of such nanostructures is enabled by the tunneling of electrons through an inversion region, from the valence band of lower potential region to the conduction band of higher potential region under an external field. The band gaps of nanostructures on the higher and lower potential regions, however, remain equal, similar to the well-known homojunction structures formed between two semiconductors with the same band gap.

Figure 1 shows the cross sections of GaN NWs and SCNTs hereby considered, which are periodic in the z axis and have [10−10] facets directed toward vacuum space in the x-y plane. The uniform electric field, modeled as a sawtooth-like potential, is in the x direction perpendicular to a [10−10] facet, as shown with an arrow in Fig. 1. For convenience, we name the nanowires as W2 and W3, as they consist of two and three coaxial hexagonal layers, respectively. Similarly, the SCNTs are named as T2r, T2R, and T3, where T2r and T2R consist of two and T3 consists of three hexagonal atomic layers, and T2r has a smaller outer diameter compared to T3 and T2R. The H-saturated SCNTs, which corresponds to T2r and T2R, are named as T2rH and T2RH, respectively. The calculations were done within the generalized gradient approximation (GGA) (Ref. 25) of density-functional theory by using the projector augmented-wave pseudopotentials[26] and a plane-wave basis set, as implemented in VASP code.[27,28] We used a kinetic-energy cutoff of 400 eV and a gamma centered uniform k-point grid of $1\times1\times7$. The fact that the plane-wave basis set describes the wave function equally well far from the atomic centers has a critical advantage in this type of calculations because, as the external field approaches the threshold field, the tail of the conduction-band wave function extends far away from the crystal structure into the vacuum toward the higher potential region in the simulation cell. Therefore, the conventional atom-centered basis sets would fail to describe the delocalized wave function in such cases. This behavior of the wave function under an external electric field also requires a relatively large vacuum space to be used. In our calculations the vacuum space is about 12 Å, which was found to be sufficient to avoid unwanted interactions.

We first analyze the atomic structure of GaN nanostructures with and without external field. Calculations show that, as the thicknesses of SCNTs and NWs decrease, their lattice constants along the periodic direction (0001) increase. The

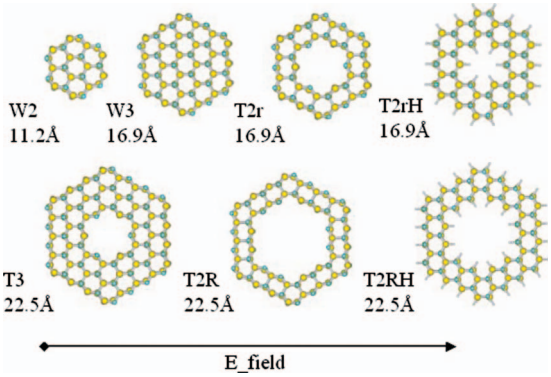

FIG. 1. (Color) Cross-sectional view of NW (W2 and W3) and SCNT (T2r, T2R, T3, T2rH, and T2RH) nanostructures, and their corresponding diameters. The arrow shows the direction of applied transverse electric field.

lattice constants of W3, W2, T3 and T2r (T2R) are calculated to be 5.32, 5.33, 5.34, and 5.35 (5.35) Å, respectively, as compared to the calculated bulk lattice constant (5.19 Å) in this direction. Nonetheless, as the surface-to-volume ratio increases, the average of bond distances decreases. For example, the average bond distance of T2r is about 0.01 Å shorter than that of T3. Under the external electric fields, on the other hand, the average of the bond distances becomes slightly larger, and the bonds in the lower potential regions are somewhat longer than those in the higher potential regions. For example, for T2r under the external field of

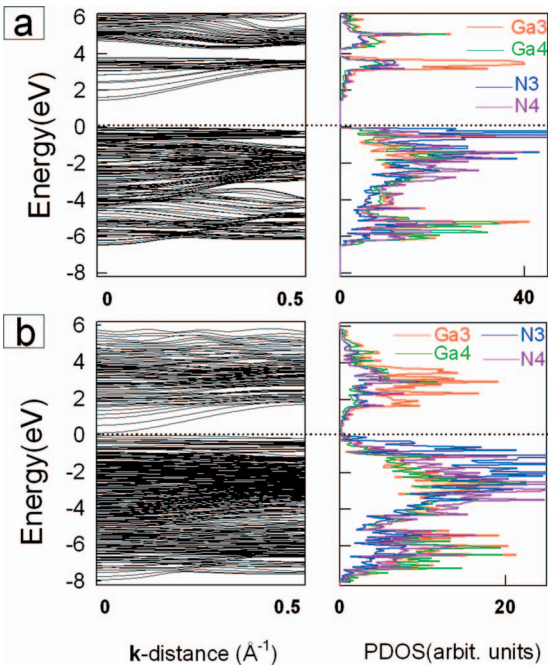

FIG. 2. (Color) Band structure and PDOS of three- and four-coordinated Ga and N atoms of T2R nanotube under (a) zero and (b) 0.42 V/Å. The red and green colors represent the PDOS of three-and four-coordinated Ga atoms, respectively, and the blue and dark-pink colors represent the PDOS of three- and four-coordinated N atoms, respectively. The Fermi level (dotted line) is set to the highest occupied state at the zero energy level.

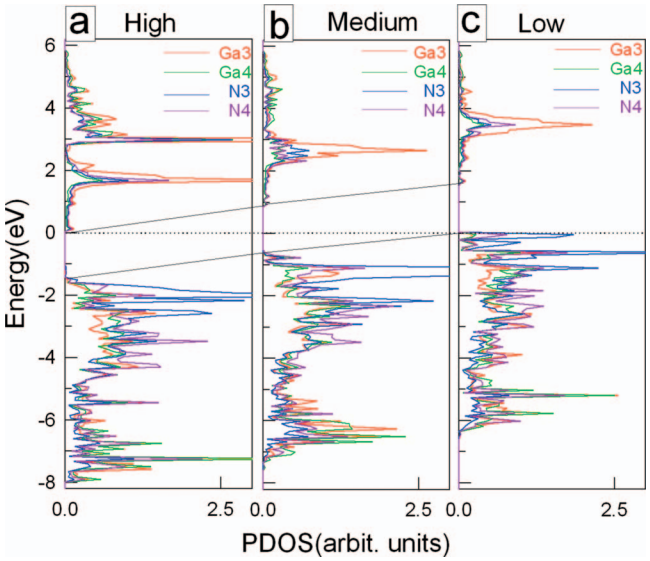

FIG. 3. (Color) The PDOS of Ga and N atoms at (a) the high potential region, (b) the medium potential region, and (c) the low potential region for T2R nanotube under 0.42 V/Å. The red and green colors represent the PDOS of three-and four-coordinated Ga atoms, respectively, and the blue and dark-pink colors represent the PDOS of three- and four-coordinated N atoms, respectively. The Fermi level is shown by a dotted line. At the higher and lower potential regions, the three-coordinated Ga and N atoms are chosen at the outermost facets of the walls, which are perpendicular to the external field (see Fig. 1 for the field direction), and the four-coordinated atoms are neighbor to these three-coordinated atoms in the walls. Similarly, for the medium potential region, the three-coordinated and their four-coordinated neighbor Ga and N atoms are chosen from one of the two edges in between the higher and lower potential regions.

0.9 V/Å, which is the threshold field for T2r, the average bond distances in the lower and higher potential regions are 1.971 and 1.968 Å, respectively.

Taking T2R as an example, we now examine the effects of the transverse electric field on the electronic properties of GaN nanostructures. Figure 2 presents the band structure and the partial density of states (PDOS) of three- and four-coordinated N and Ga atoms under zero and 0.42 V/Å electric fields. For unsaturated GaN nanostructures, the three-coordinated N and Ga surface atoms introduce midgap states at the top of the valence and below the conduction bands, respectively. While N contribution mainly comes from *p* states, Ga contribution is from *p*, *d*, and *s* states (in order of their contribution). The band gap between these midgap states, which is about 1.45 eV for T2R, closes when the magnitude of the external field reaches the threshold value, i.e., 0.42 V/Å [Fig. 2(b)].

However, analyzing the PDOS of Ga and N atoms in the higher and lower potential regions, it can be seen that (Fig. 3) the band-gap closure observed in Fig. 2(b) is not a simple semiconductor-metal transition, but rather it is an induction of a junction across the diameter. This junction forms as a result of the relative reduction in energy of the electronic states in the higher potential region with respect to the energy of those states in the lower potential region, so that the

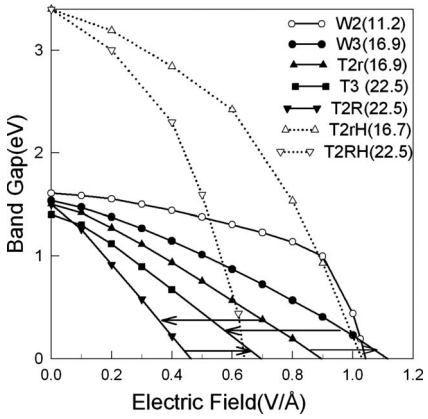

FIG. 4. Band gap as a function of electric field for SCNTs and NWs. The solid and dotted lines correspond to the unsaturated and H-saturated structures, respectively. The right and left arrows indicate the increasing threshold electric field with increasing the wall thickness, and the decreasing threshold field with increasing the diameter, respectively. The threshold electric fields for the gap closure are estimated by extrapolating the data points to zero band gap.

valence-band maximum (VBM) on one side is leveled to the conduction-band minimum (CBM) on the opposite side. The band gap of the nanostructures on the both sides, on the other hand, remains constant, resembling a homojunction formed at the interface of two semiconductors with the same band gap but with different (initial) Fermi levels. In such a structure, the transport of electrons under electric field, from the valence band of the lower potential region to the conduction band of the higher potential region, occurs via tunneling.[29,30] Consequently, under a further electric field in the axial direction, the conductivities of such nanostructures in the higher and lower potential regions will involve electron and hole charge carriers, respectively. Further examining the electronic density of states (DOS) in the higher and lower potential regions [Figs. 3(a) and 3(c)], and comparing to the unperturbed DOS [Fig. 2(a)], it can be seen that the conduction band in the lower potential region is almost totally shifted to the higher potential region (with the exception of surface states). However, the shape of the valence band on the higher and lower potential regions remains mostly unchanged, except that the intensity of the electronic states at the top of the valence band of the lower potential region is somewhat increased. Such variations in the local DOS under a transverse electric field may also affect the optical properties of these nanostructures. Although the previous *ab initio* calculations on CNT (Refs. 16–18) and BNNT (Refs. 19 and 20) have also shown the localization of highest occupied molecular orbital and lowest unoccupied molecular orbital states at the lower and higher potential regions, they have concluded the emergence of a semiconductor-metal transition under a transverse electric field. Therefore, the results presented hereby provide a better understanding of the electronic properties of semiconducting nanostructures, in general, under an external electric field.

To analyze the dependence of the threshold electric field on the diameter and the wall thickness, in Fig. 4 we plot the band gap of the nanostructures as a function of the electric field. We remind that the band gaps considered here are between the VBM and CBM at the lower and higher potential regions across the diameter, respectively. In general, under the small electric fields the band-gap tuning rate is slow; however, as the electric field strengths increase the band-gap tuning shows a linear behavior with respect to the electric field.[31] This happens because initially delocalized charge density quickly responds to the electric field and localizes in the higher potential region. The increased kinetic energy of this localized charge density, then, somewhat compensates for the decrease in the potential energy in this region. Under higher electric fields, however, as the difference between the potential energy of the electronic states in the higher and lower potential regions becomes larger, the contribution of the kinetic energy becomes less important. As a result, the band-gap reduction shows a linear dependence on the electric field. Another feature shown in Fig. 4 is that the unperturbed band gaps of H-saturated SCNTs (T2rH and T2RH) are much larger than those of the corresponding unsaturated SCNTs (T2r and T2R). In the GGA approximation[25] used here, the band gap of wurtzite (bulk) GaN was calculated to be 1.95 eV, which is underestimated relative to the experimentally measured band gap, i.e., 3.50 eV.[32] Compared to the bulk band gap, while the band gaps of the unsaturated GaN nanostructures are reduced ($\sim$1.45 eV) due to midgap states created by the surface dangling bonds, the band gaps of the H-saturated structures are greatly enhanced ($\sim$3.4 eV) by the strong confinement effects at these small sizes. This enlargement in the band gap of H-saturated SCNTs was also observed experimentally through their optical spectrum.[9]

In Fig. 4, the threshold electric fields are obtained by extrapolating the data points to zero band gaps. As it can be followed in the figure, for the structures of the same outer diameter, when the wall thickness is increased the threshold electric field also increases (shown by right directed arrows). On the other hand, for the structures with the same wall thickness, when the diameter is increased the threshold field decreases substantially (shown by left directed arrows). Since the threshold electric field is more sensitive to the diameter than the wall thickness, it decreases even when the diameter and the wall thickness are increased simultaneously, i.e., from T2r to T3. Therefore, for the experimental realization of semiconductor-homojunction induction with practical fields, one should prefer SCNTs with small wall thicknesses and large diameters. Taking into account the decreasing rate of the threshold fields with the diameter, we estimate the threshold field of 10 nm diameter unsaturated SCNTs with two- and three-atomic layer wall thicknesses to be about 0.012 and 0.05 V/Å, respectively. These fields are already in the experimentally accessible range. The threshold fields of H-saturated SCNTs, on the other hand, are somewhat larger than those of corresponding unsaturated SCNTs.

The threshold electric fields calculated here for GaN nanostructures are comparable to those of semiconducting CNTs (Refs. 16 and 17) obtained from density-functional studies. However, it should be taken into account that the band gaps hereby calculated, in the GGA approximation, are underestimated as stated above. Therefore, the threshold electric fields calculated here should be smaller than the actual values. For example, the band gaps and threshold fields

of ZGNRs, calculated within the pure density-functional approximations,[21,22,33] were shown to be much smaller than the corresponding values calculated within the hybrid functionals,[22–24,33] such as B3LYP.[34] Hybrid functionals, which include a fraction of Hartree-Fock exchange energy, are known to provide better band gaps compared to pure functionals.[35]

For a homojunction to be formed, the potential drop in the SCNTs and NWs must be equal or higher than their band gaps to induce a full band bending across the nanostructures. However, when the nanostructures contain *p*- or *n*-type impurities, the potential in the nanostructures and the band bending depend on the contact type and the direction of the applied bias through the contact interface. In this regard, for the metal contacts only a "reverse bias" can induce a sufficiently high potential to induce a full band bending. An example of this is the Zener diode,[29] for which—depending on the bias—the CBM can be at the same level or lower than the VBM. In the case of oxide contacts, on the other hand, a full band bending may never take place as the charge density at the interface, which screens the external bias, increases rapidly for the biases above a certain threshold value. Nevertheless, when the nanostructures are heavily doped with the deep donor or acceptor impurities, under the large gate voltages the energy difference between the CBM and VBM can be as small as room temperature.

In conclusion, using density-functional theory calculations, we have studied the electronic properties of GaN SCNTs and NWs under the transverse electric fields and showed that the electric field induces a homojunction across the diameter of the nanostructures. The conduction in these nanostructures, which would be initiated by tunneling of electrons from the valence band in the lower potential region to the conduction band in the higher potential region under the transverse electric fields, involves electron and hole charge carriers in the high and low potential regions, respectively. For practical applications, GaN SCNTs with large diameters and small wall thicknesses should be preferred, as they require smaller electric fields.

This research project was carried out under the auspices of the Institute for Functional Nanomaterials (NSF Grant No. 0701525). This research was also supported in part by NASA Cooperative Agreement No. NNX07AO30A (PR NASA EPSCoR) and Department of Energy Grant No. DE-FG02-08ER46526 (PR DOE EPSCoR). The authors gratefully acknowledge the High Performance Computing Facilities (HPCF) provided by the University of Puerto Rico.

[1] V. N. Tondare, C. Balasubramanian, S. Shende, D. S. Joag, V. P. Godbole, S. V. Bhoraskar, and M. Bhadbhade, Appl. Phys. Lett. **80**, 4813 (2002).
[2] A. Loiseau, F. Willaime, N. Demoncy, G. Hug, and H. Pascard, Phys. Rev. Lett. **76**, 4737 (1996).
[3] J.-R. Kim, H. M. So, J. W. Park, J.-J. Kim, J. Kim, C. J. Lee, and S. C. Lyu, Appl. Phys. Lett. **80**, 3548 (2002).
[4] C. Y. Nam, D. Tham, and J. E. Fischer, Appl. Phys. Lett. **85**, 5676 (2004).
[5] B. S. Simpkins, L. M. Ericson, R. M. Stroud, K. A. Pettigrew, and P. E. Pehrsson, J. Cryst. Growth **290**, 115 (2006).
[6] B.-S. Xu, L.-Y. Zhai, J. Liang, S.-F. Ma, H.-S. Jia, and X.-G. Liu, J. Cryst. Growth **291**, 34 (2006).
[7] Y. Yang, V. J. Leppert, S. H. Risbud, B. Twamley, P. P. Power, and H. W. H. Lee, Appl. Phys. Lett. **74**, 2262 (1999).
[8] T. W. Weeks, Jr., M. D. Bremser, K. S. Ailey, E. Carlson, W. G. Perry, and R. F. Davis, Appl. Phys. Lett. **67**, 401 (1995).
[9] J. Goldberger, R. He, Y. Zhang, S. Lee, H. Yan, H.-J. Choi, and P. Yang, Nature (London) **422**, 599 (2003).
[10] S. C. Hung, Y. K. Su, S. J. Chen, L. W. Ji, T. H. Fang, L. W. Tu, and M. Chen, Appl. Phys. A: Mater. Sci. Process. **80**, 1607 (2005).
[11] B. D. Liu, Y. Bando, C. C. Tang, G. Z. Shen, D. Golberg, and F. F. Xu, Appl. Phys. Lett. **88**, 093120 (2006).
[12] Y. Huang, X. Duan, Y. Cui, and C. M. Lieber, Nano Lett. **2**, 101 (2002).
[13] S. J. Tans, A. R. M. Verschueren, and C. Dekker, Nature (London) **393**, 49 (1998).
[14] R. Martel, T. Schmidt, H. R. Shea, T. Hertel, and P. Avouris, Appl. Phys. Lett. **73**, 2447 (1998).
[15] T. Tanaka, H. Jin, Y. Miyata, S. Fujii, H. Suga, Y. Naitoh, T. Minari, T. Miyadera, K. Tsukagoshi, and H. Kataura, Nano Lett. **9**, 1497 (2009).
[16] J. O'Keeffe, C. Wei, and K. Cho, Appl. Phys. Lett. **80**, 676 (2002).
[17] A. Rochefort, M. D. Ventra, and P. Avouris, Appl. Phys. Lett. **78**, 2521 (2001).
[18] L.-G. Tien, C.-H. Tsai, F.-Y. Li, and M.-H. Lee, Phys. Rev. B **72**, 245417 (2005).
[19] K. H. Khoo, M. S. C. Mazzoni, and S. G. Louie, Phys. Rev. B **69**, 201401(R) (2004).
[20] C.-C. Chen, M.-H. Lee, and S. J. Clark, Nanotechnology **15**, 1837 (2004).
[21] Y.-W. Son, M. L. Cohen, and S. G. Louie, Nature (London) **444**, 347 (2006).
[22] E. Rudberg, P. Salek, and Y. Luo, Nano Lett. **7**, 2211 (2007).
[23] O. Hod, V. Barone, J. E. Peralta, and G. E. Scuseria, Nano Lett. **7**, 2295 (2007).
[24] E.-J. Kan, Z. Li, J. Yang, and J. G. Hou, Appl. Phys. Lett. **91**, 243116 (2007).
[25] J. P. Perdew, K. Burke, and M. Ernzerhof, Phys. Rev. Lett. **77**, 3865 (1996).
[26] G. Kresse and D. Joubert, Phys. Rev. B **59**, 1758 (1999).
[27] G. Kresse and J. Hafner, Phys. Rev. B **48**, 13115 (1993).
[28] G. Kresse and J. Hafner, Phys. Rev. B **49**, 14251 (1994).
[29] C. Zener, Proc. R. Soc. London, Ser. A **145**, 523 (1934).
[30] S. Glutsch, Phys. Rev. B **69**, 235317 (2004).
[31] W2 wire is an exception in this case, for which the band gap declines sharply around 0.95 V/Å. A test calculation performed with an energy cutoff of 500 eV and a k mesh of $1\times1\times9$ in a larger supercell (about 14 Å vacuum space) gives similar results.
[32] B. Monemar, Phys. Rev. B **10**, 676 (1974).
[33] V. Barone, O. Hod, and G. E. Scuseria, Nano Lett. **6**, 2748 (2006).
[34] A. D. Becke, J. Chem. Phys. **98**, 5648 (1993).
[35] J. Paier, M. Marsman, K. Hummer, G. Kresse, I. C. Gerber, and J. G. Angtan, J. Chem. Phys. **124**, 154709 (2006).